Electron Technology, 2, 2/3, pp. 139–147. Institute of Electron Technology P.A. Sci., Warsaw 1969

STATISTICAL NATURE OF THE INFRARED HETERODYNE SIGNAL[1]

Statystyczny charakter sygnału heterodyny w podczerwieni

La nature statistique d'un signal hétérodyne infrarouge

Статический характер инфракрасного гетеродинного сигнала

M. C. TEICH
Columbia University, New York, U.S.A.

1. INTRODUCTION

HETERODYNE detection is a process which has been used in the radiowave, microwave, and optical regions of the electromagnetic spectrum. Recently, the technique has been extended to the middle infrared as well [1–3]. This paper discusses theoretical and experimental considerations related to the signal-to-noise ratio and the statistical nature of the coherently detected signal at the 10.6 μm CO_2 laser wavelength.

Coherent detection differs in several significant respects from direct detection, or simple photon counting. In particular, the increased sensitivity available through its use in the infrared allows the detection of far weaker signals than by means of other techniques. In the submillimeter region, an improvement in sensitivity with heterodyne operation has been demonstrated for InSb, pyroelectric, and Golay cell detectors. Using techniques similar to those described here, coherent detection experiments have been previously reported in the visible and the near infrared with photoemissive devices, photodiodes, and photoconductors.

The operation of the heterodyne receiver is made possible by the "nonlinear" response of the photodetector to the incident total radiation field. Two electromagnetic waves of different frequencies (ω_1 and ω_2) mix at the photodevice and produce an electrical signal at the difference frequency ($\omega_1-\omega_2$). When one of these beams is made to be strong (if it is locally produced, it is then called the local oscillator or LO), the sensitivity for the process is considerably increased over the straight detection (video) case because of the high conversion gain between power at the input and at the difference frequencies. In addition to this high conversion gain, the heterodyne detector exhibits both strong directivity and frequency selectivity. It is the frequency selectivity of the coherent detection

[1] This work was supported by the National Science Foundation of the United States of America.

process which permits the noise bandwidth to be reduced to a very small value. The heterodyne detector is linear only insorfar as the detector output *power* is proportional to the input signal radiation *power*.

At optical and infrared frequencies, the heterodyne detector acts as both an antenna and a receiver, and has an integrated effective aperture limited by approximately λ^2. Careful alignment between the LO and signal beams is necessary in order to maintain a constant phase over the surface of the photodetector. The use of coherent detection in a communications system is therefore limited by the atmospheric distortion of the wavefront, which imposes a restriction on the maximum achievable signal-to-noise ratio. Heterodyne detection is consequently most useful for detecting weak signals which are coherent with a locally produced source. It should be mentioned that the coherent detection technique is also capable of furnishing information about the frequency spectrum of a signal beam.

In the case where both the signal and the LO derive from the same source (such as in the experiments described in this paper), the heterodyne signal can provide information about the velocity of a target through the Doppler shift. This is also possible if the LO and signal beams arise from different, but frequency locked lasers. Heterodyne detection is also useful for heterodyne spectroscopy, and in the study of physical processes occurring in materials. Use of the technique has already been made in the design of a laser Doppler velocimeter, which measures localized flow velocities in gases and liquids.

It is the availability of the high radiation power from the CO_2 laser, coupled with the 8 to 14 μm atmospheric window, which make sensitive detection at 10.6 μm important for systems use. Furthermore, it is at these longer wavelengths where the higher sensitivity available from coherent detection is particularly valuable, since the user may discriminate against various noise sources including the blackbody radiation from objects at room temperature, which is appreciable at 10.6 μm. In the experiments reported below, a minimum detectable radiation power which is within a factor of 5 of the theoretical quantum limit has been observed.

Because the setup employed in these experiments detects the scattered radiation from a diffusely reflecting moving surface, it is, in effect, a prototype CO_2 laser radar. The statistical behavior of the heterodyne signal relates to the nature of the scatterer, and is important for considerations pertinent to optimum signal processing.

2. THEORY

A generalized schematic of the optical or infrared (absorption) heterodyne receiver [1–3] is shown in Fig. 1. The photodetector responds to the positive-frequency portion of the electric field operator E^+. The heterodyne signal may be expressed in terms of Glauber's first-order correlation functions [1, 4, 5]. Neither sum nor double-frequency components appear at the output of the quantum-mechanical absorption detector, regardless of its response time. Only the difference frequency appears when $h\nu \gg kT$, where $h\nu$ is the photon energy and kT is the thermal excitation energy of the detector. For stationary constituent beams, and precise first-order coherence of the incident total radiation field, optimum photomixing will occur [1, 5]. For this case, the minimum detectable powers

(MDP) are given by $h\nu\Delta f/\eta$ for the photoemitter and reverse-biased photodiode, and by $2h\nu\Delta f/\eta$ for the photoconductor and photovoltaic diode [1]. Here Δf is the receiver bandwidth and η is the detector quantum efficiency.

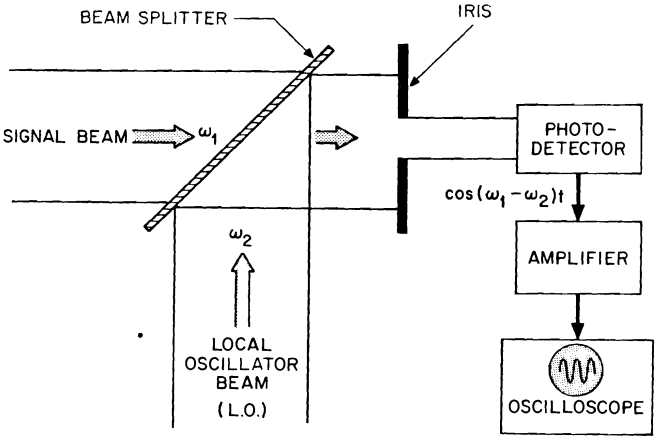

FIG. 1. The generalized infrared or optical heterodyne receiver.

3. EXPERIMENT

A particular advantage of the heterodyne technique is the ability to detect very low radiation powers. A plot of the minimum detectable number of photons vs. the frequency of electromagnetic radiation from radiowave to x-rays at the present state-of-the-art is

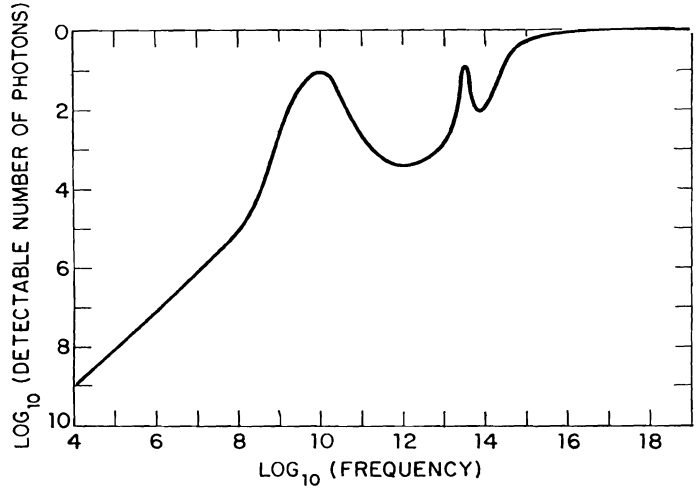

FIG. 2. Minimum detectable number of photons vs frequency from radiowaves to X-rays.

given in Fig. 2. The peak in the curve at $\log_{10}\nu \approx 13.45$ corresponds to near-optimum detection at 10.6 μm as reported here. In Fig. 3, an artist details the structure of a lead-tin chalcogenide infrared photovoltaic diode detector. This device is similar to those

used in the heterodyne experiments described here and elsewhere [1–3]. Details pertinent to their operation have been given by Melngailis [6]. It is noted that the relative lead-tin composition may be chosen so as to peak the response at any desired wavelength in the

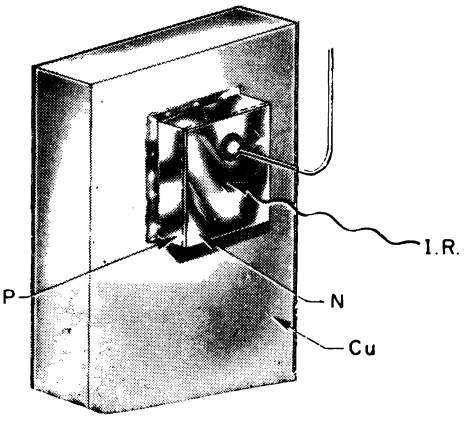

FIG. 3. Structure of a lead-tin telluride photovoltaic detector diode.

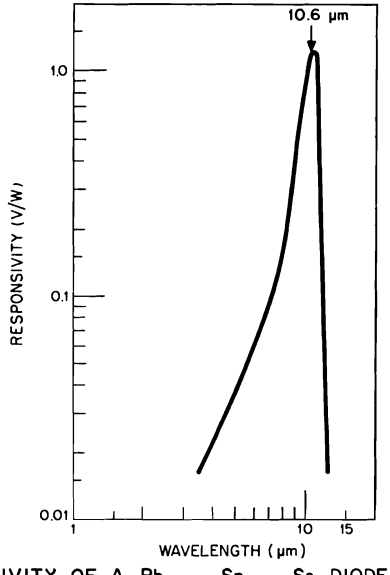

FIG. 4. Responsivity of a $Pb_{0.936}Sn_{0.064}Se$ diode as a function of wavelength at 77°K.

middle infrared. The responsivity of a $Pb_{0.936}Sn_{0.064}Se$ diode at 77°K is shown in Fig. 4. It has been designed to reach a maximum value at the CO_2 laser wavelength. By improved fabrication techniques and by chemical etching, the responsivity may be increased by at least a factor of 3 over the curve presented in Fig. 4. $Pb_{1-x}Sn_xTe$ detectors have been produced with considerably higher responsivities and with reverse impedances which are of

the order of 100 ohms [6]. Both lead-tin selenide and lead-tin telluride have been used in the heterodyne mode of operation [1].

The experimental arrangement for infrared heterodyne measurements with a photovoltaic lead-tin chalcogenide detector is illustrated in Fig. 5. The radiation from a CO_2-N_2-He laser, emitting approximately 10 Watts at 10.6 μm, was incident on a modified Michelson interferometer. One mirror of the conventional interferometer was replaced by an off-center rotating aluminum wheel with a roughened surface. The diffusely scat-

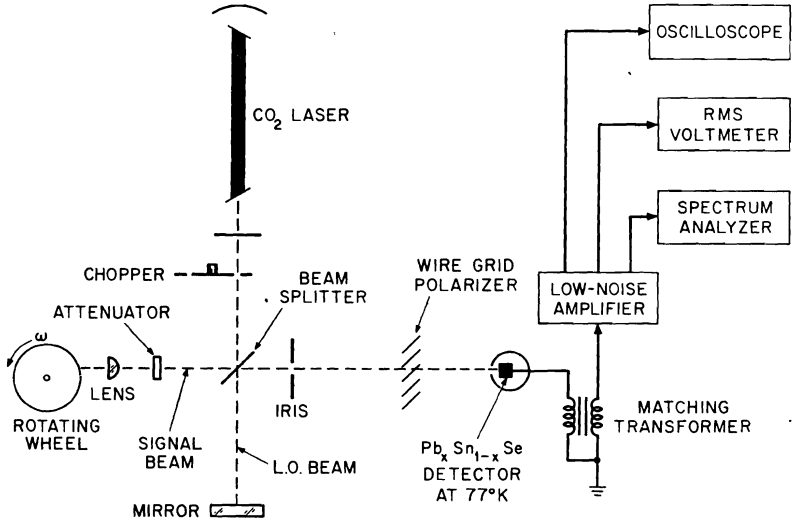

FIG. 5. Experimental arrangement for heterodyne measurements with a lead-tin selenide photovoltaic detector.

tered radiation from the wheel provided a Doppler-shifted signal which was recombined at the beam splitter with the unshifted LO radiation reflected from the mirror of the other interferometer leg. The beam splitter was cocked at a slight angle to 45° in order to prevent this reflected radiation from feeding back into the laser.

The experimental setup, with the exception of the rotating wheel and the chopper, was mounted on a granite slab supported by compressed fiberglass blocks. To further minimize the effect of acoustic vibrations, the 1.25-m-long sealed laser tube was enclosed in a shield constructed of acoustic tile. The laser was operated well above threshold and was tuned to operate on a single line and mode. An uncoated Kodak Irtran II flat (of thickness 0.64 cm) served as a beam splitter, and front surface mirrors were of standard aluminum-coated glass. A 2.54-cm-focal-length Irtran II lens inserted in the signal beam focused the radiation to a single point on the rim of the rotating wheel. The function of the lens was to collect sufficient scattered radiation to permit an incoherent (nonheterodyne) measurement of the scattered signal power at the detector for calibration purposes, and to insure spatial coherence of the scattered radiation at the detector. Irises were used to maintain the angular alignment of the wave fronts of the two beams to $\sim$ 2 mrad, which is well within the required angular tolerance for optimum photomixing

($\lambda/\alpha \sim 5$ mrad for a detector aperture $\alpha = 2$ mm). A Perkin-Elmer wire-grid polarizer insured that the recombined beams had a common linear polarization. The detector output is transformed up in impedance to 50 ohms, and them amplified and displayed.

We outline the principle results obtained from such experiments and then present data pertinent to the discussion of the statistical nature of the signal. A multiple-sweep display of the heterodyne signal in $Pb_{1-x}Sn_xSe$ as seen on a Tektronix type 585 A oscilloscope is shown in Fig. 6*a*. The loss of definition of the waveform in the fifth cycle reflects the finite bandwidth of the signal, as discussed later. A single sweep of the same signal,

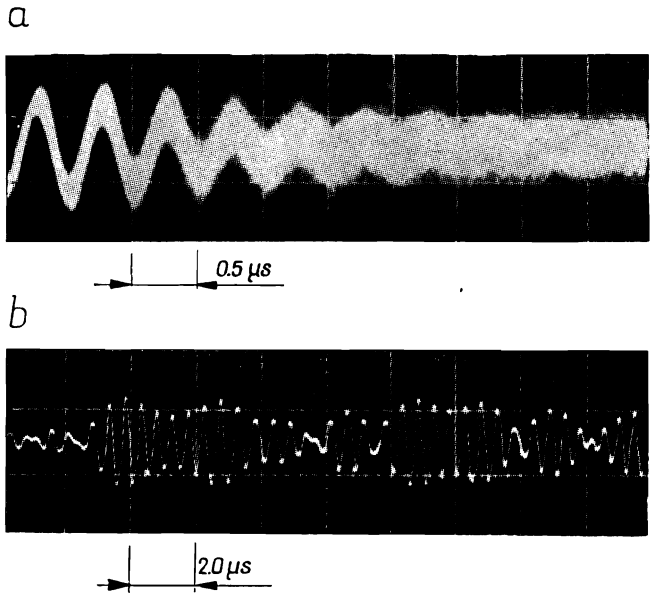

FIG. 6. Oscilloscope displays of the heterodyne signal.

but with a longer time scale, is shown in Fig. 6*b*. The modulation of the signal envelope arises from the random nature of the scattering surface. The data points representing the observed signal-to-noise ratio of the heterodyne signal for a typical run for a given signal-beam radiation power P_s are given in Fig. 7. The theoretical curve, $(S/N)_{\text{power}} = \eta P_s/2h\nu\Delta f$, is in good agreement with the data. The heterodyne signal is at 2.05 MHz and the detection bandwidth is 10 MHz, giving a minimum detectable power of 7.6×10^{-12} Watt. The signal-to-noise measurements were effected using a Hewlett-Packard type 3400 A RMS voltmeter.

The time trace of a typical heterodyne signal and its envelope are represented in Fig. 8. The probability density of the signal envelope may be obtained by sampling. Due to random scattering centers, the laser radiation scattered from the rotating Doppler wheel (which has a granularity ~ 10 μm) may be considered to possess a Gaussian distribution of electric field. Beating with an amplitude-stabilized coherent local oscillator without fluctuation, the heterodyne voltage is expected to accurately reflect this distribution.

For a focused spot of diameter d on the wheel, a completely new area of the wheel is illuminated every d/v seconds, giving scattered radiation uncorrelated with that of the

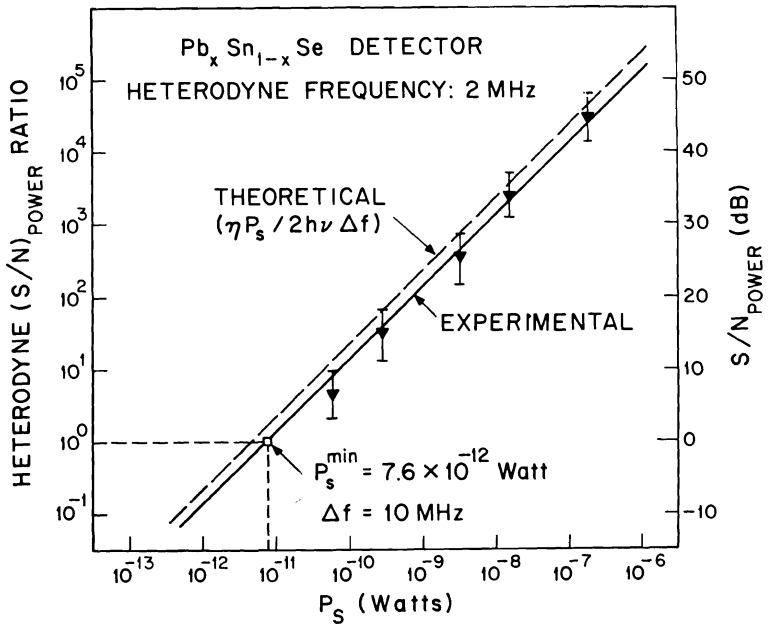

FIG. 7. Experimental and theoretical signal-to-noise ratios as a function of signal-beam power.

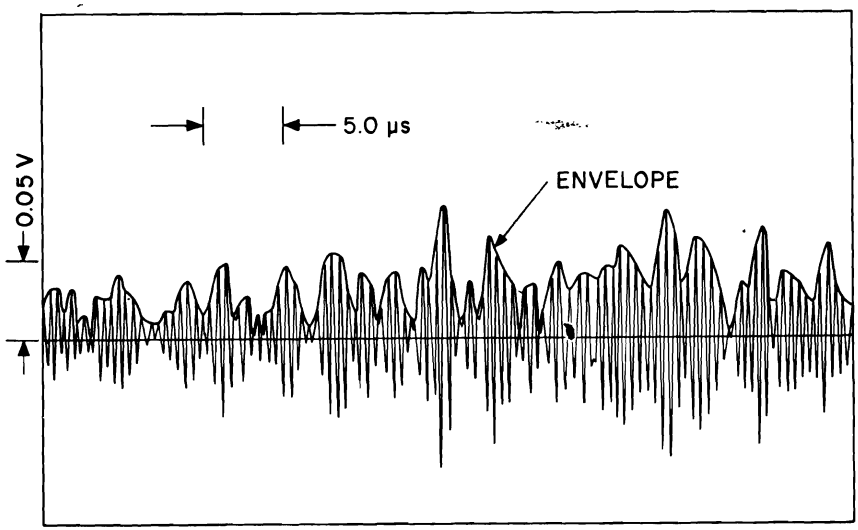

FIG. 8. Time trace of a typical heterodyne signal and its envelope.

previous time interval. With the wheel velocity v given by $v = r\dot{\theta}$ and $d \sim F\lambda/D$ ($\dot{\theta}$ is the angular velocity of the wheel $= 120\pi$ sec^{-1}, r its radius $= 5.05$ cm, F the focal length of the lens $= 2.54$ cm, and D the radiation beam diameter ≈ 0.5 cm), the heterodyne signal bandwidth B is given by $B \approx r\dot{\theta}D/F\lambda$. The ratio of bandwidth to heterodyne frequency is independent of $\dot{\theta}$ and depends only on geometrical factors. The narrowband

character of the signal (bandwidth less than heterodyne frequency) was preserved in all experiments performed, as may be seen in the relative power spectral density curve displayed in Fig. 9. The observed bandwidth of approximately 0.4 MHz is in good agreement

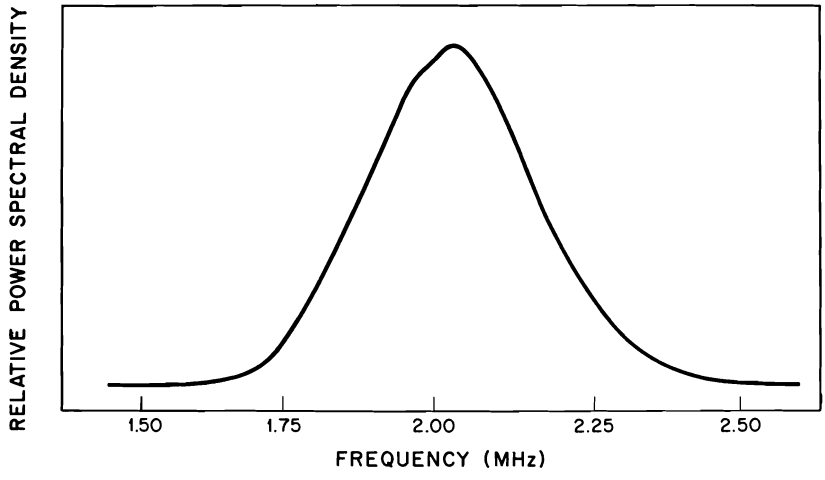

FIG. 9. Power spectral density of the heterodyne signal as a function of frequency.

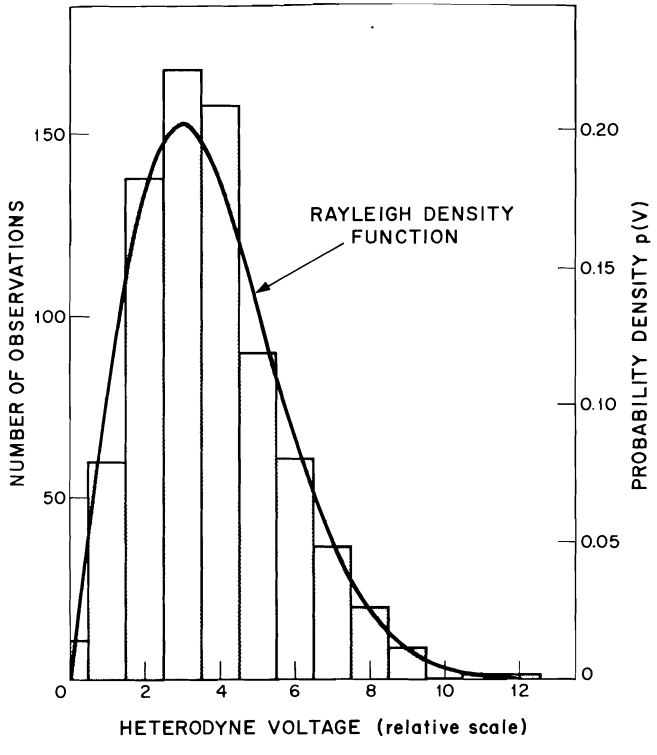

FIG. 10. Probability density of the heterodyne voltage envelope vs heterodyne voltage.

with the expected value obtained from the expression given above. Measurement of the power spectral density was made with a Panoramic type SPA-3a spectrum analyzer.

Finally, the experimental probability density $p(V)$ of the heterodyne voltage envelope vs. the heterodyne voltage is presented in Fig. 10. The distribution is fit very well by a Rayleigh density function, as would be expected for the envelope of a narrowband Gaussian random process. A chi-squared test gave a value of $\chi^2 = 8.28$ with 7 degrees of freedom, giving a probability $P = 0.3$ that the deviations from the Rayleigh density function would be expected to be greater than those here observed. Thus it appears that the signal envelope may indeed be fit by a Rayleigh distribution.

This result is of importance for optimum processing of an infrared heterodyne signal from a known scatterer. Alternatively, information may be obtained about an unknown scatterer from an examination of the statistics of the heterodyne signal. Related observations have been made in the visible by GOULD et al. [7], who observed a heterodyne signal using radiation scattered by a piece of white bond paper.

4. CONCLUSION

Heterodyne techniques, which have been used extensively in the radiowave and microwave regions, and more recently in the optical (visible) portion of the electromagnetic spectrum, are equally as valuable in the infrared. The availability of the high power CO_2 laser, coupled with the 8 to 14 μm atmospheric window, is expected to make the infrared heterodyne receiver important for communications applications. It is more sensitive than the optical heterodyne receiver because of the smaller photon energy (the minimum detectable power is proportional to the photon energy). The envelope of the infrared heterodyne signal obtained from a scatterer producing a Gaussian electric-field distribution is Rayleigh distributed. This result is consistent with expectations.

Acknowledgement. I would like to thank Professors W. R. BENNETT and E. N. PROTONOTARIOS for helpful conversations pertaining to random processes.

REFERENCES

1. M. C. TEICH, in *Semiconductors and Semimetals*, edited by R. K. WILLARDSON and A. C. BEER (Academic Press, Inc., New York, 1970), **5**, *Infrared Detectors*.
2. M. C. TEICH, Proc. IEEE, **56**, 37, 1968; Proc. IEEE, **57**, 786, 1969.
3. M. C. TEICH, R. J. KEYES, and R. H. KINGSTON, Appl. Phys. Letters, **9**, 357, 1966.
4. R. J. GLAUBER, in *Quantum Optics and Electronics*, edited by C. DE WITT, A. BLANDIN, and C. COHEN-TANNOUDJI (Gordon and Breach Science Publishers, Inc., New York, 1965), p. 65.
5. M. C. TEICH, Appl. Phys. Letters, **14**, 201, 1969.
6. I. MELNGAILIS and T. C. HARMAN, in *Semiconductors and Semimetals*, edited by R. K. WILLARDSON and A. C. BEER (Academic Press, Inc., New York, 1970), **5**, *Infrared Detector*.
7. G. GOULD, S. F. JACOBS, J. T. LATOURRETTE, M. NEWSTEIN, and P. RABINOWITZ, Appl. Optics, **3**, 648, 1964.